

Aberrant Retinal Projections in Congenitally Deaf Mice: How Are Phenotypic Characteristics Specified in Development and Evolution?

DEBORAH L. HUNT,^{1,2} BRYAN KING,¹ DIANNA M. KAHN,¹
EBENEZER N. YAMOAHA,^{1,3} GARY E. SHULL,⁴ AND LEAH KRUBITZER^{1,2*}

¹Center for Neuroscience, University of California at Davis, Davis, California

²Department of Psychology, University of California at Davis, Davis, California

³Department of Otolaryngology, University of California at Davis, Davis, California

⁴Department of Molecular Genetics, Biochemistry, and Microbiology, University of Cincinnati, College of Medicine, Cincinnati, Ohio

ABSTRACT

The contribution of sensory input to the formation of sensory system-specific (sensoritopic) connections of the thalamus and midbrain was investigated using mice lacking the Na⁺-K⁺-2Cl⁻ cotransporter (NKCC1) or the plasma membrane Ca²⁺-ATPase isoform2 (PMCA2). Because these mice are congenitally deaf, the developing nervous system has no exposure to sensory-driven neural activity from the auditory system. Here we compared the retinofugal pathway in normal and congenitally deaf mice using intraocular injections of neuroanatomical tracers into each eye, and relating tracer patterns to identified thalamic nuclei and superior colliculus layers. We demonstrate that loss of such activity results in aberrant projections of the retina into nonvisual auditory structures such as the medial geniculate nucleus and the intermediate layers of the superior colliculus. These findings indicate that activity from peripheral sensory receptor arrays is necessary not only for the refinement of developing connections within a unimodal structure, but for the establishment of sensoritopic or sensory-specific connections of unimodal and multimodal structures. We hypothesize that specification of such connections may occur through the modulation of spatial expression patterns of molecules known to be involved in the development of topography of connections between brain structures, such as the ephrins, via activity-dependent, CRE-mediated gene expression.
© 2005 Wiley-Liss, Inc.

Key words: development; evolution; lateral geniculate; medial geniculate; retinofugal

The mammalian brain is capable of remarkable reorganization during development and throughout the life of an individual. A variety of studies, particularly on the visual system, have demonstrated that sensory experience plays a large role in shaping appropriate connection patterns in the nervous system, and that a loss or alteration of sensory receptor input can result in large organizational changes in the brain (for reviews, see Katz and Shatz, 1996; Shatz, 1996; Sur et al., 1999; Krubitzer and Kahn, 2003; Ruthazer and Cline, 2004). Indeed, with a complete loss of sensory receptor arrays or sensory-driven activity very early in development, such as in congenital blindness

or deafness, reorganization can be massive and portions of the neocortex that would normally be occupied by the lost

*Correspondence to: Leah Krubitzer, Center for Neuroscience, 1544 Newton Court, Davis, CA 95616. Fax: 530-757-8827. E-mail: lakrubitzer@ucdavis.edu

Received 16 August 2005; Accepted 17 August 2005
DOI 10.1002/ar.a.20251

Published online 2 October 2005 in Wiley InterScience (www.interscience.wiley.com).

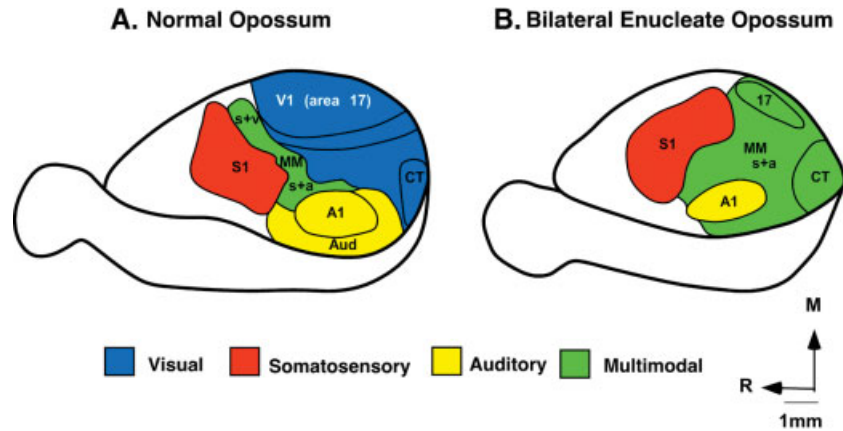


Fig. 1. The organization of the neocortex as defined using electrophysiological recording techniques combined with cortical myeloarchitecture in (A) normal opossums and (B) bilaterally enucleated opossums. Complete loss of sensory receptors, as in the bilaterally enucleated opossums, or a large reduction in sensory-driven activity from a particular sensory system results in a large reorganization of cortex. In bilaterally enucleated opossums, all of cortex that would normally be involved in processing visual inputs contains neurons that respond to somatosensory and auditory stimulation. The bilateral enucleations oc-

curred very early in development, well before thalamic axons reach the developing neocortex, and before retinal ganglion cells reach the diencephalons. In bilaterally enucleated opossums, the architectonic features of area A1, V1, and S1 are still maintained, although the size of cortical fields is altered. The anatomical substrate for the functional changes observed in the neocortex in these animals is not known. Rostral is to the left and medial is to the top. This figure is based on results from Kahn and Krubitzer (2002).

curated very early in development, well before thalamic axons reach the developing neocortex, and before retinal ganglion cells reach the diencephalons. In bilaterally enucleated opossums, the architectonic features of area A1, V1, and S1 are still maintained, although the size of cortical fields is altered. The anatomical substrate for the functional changes observed in the neocortex in these animals is not known. Rostral is to the left and medial is to the top. This figure is based on results from Kahn and Krubitzer (2002).

sensory system will be taken over by the remaining sensory systems (Hunt et al., 2002; Kahn and Krubitzer, 2002). This has recently been demonstrated in bilaterally enucleated *Monodelphis domestica* (Fig. 1).

Until recently, the notion that humans who develop in the absence of one sensory system (e.g., are blind or deaf) become better at making sensory discriminations with the remaining sensory systems was, for the most part, anecdotal. However, recent studies in blind individuals indicate that the capabilities of other sensory systems in some ways exceed that of sighted individuals. Using auditory event-related potentials, Röder et al. (1999) demonstrated that there is a shorter detection time for auditory discrimination tasks in blind versus sighted individuals and in a subsequent study (Röder et al., 2000), they demonstrated that blind individuals process language faster than sighted individuals. Thus, there appears to be a compensatory adaptation of the auditory system in the congenitally blind. This compensatory adaptation is likely due to changes in the nervous system at both subcortical and cortical levels. This notion is supported by recent positron emission tomography (PET) studies in blind individuals, which indicate that auditory localization activates occipital cortex in regions normally involved in visual localization and motion detection (Weeks et al., 2000). This massive cross-modal plasticity is also observed in the somatosensory system. For instance, in congenitally blind individuals, primary visual cortex is active during tactile tasks such as Braille reading (Sadato et al., 1996; Cohen et al., 1997; Büchel et al., 1998).

Similar types of cross-modal plasticity have been demonstrated in congenitally deaf humans. For instance, congenitally deaf individuals have enhanced amplitudes of the ERP's N1 component for processing of visual motion (Armstrong et al., 2002) and when attending to the peripheral visual field compared to normal individuals (Neville and Lawson, 1987). Functional imaging studies indi-

cate that auditory areas are active during visual and somatosensory tasks in congenitally deaf individuals (Catalan-Ahumada et al., 1993; Levanen et al., 1998; Finney et al., 2001; for review, see Bavelier and Neville, 2002). While these studies clearly demonstrate that cross-modal plasticity in the developing mammalian brain can be extensive, the anatomical substrate for these functional changes is not known. For example, how do the remaining sensory systems invade cortical territory normally occupied by the lost sensory system? Are these large territory shifts in the neocortex of congenitally deaf individuals the result of changes in thalamocortical connectivity and corticocortical connections, or do some alterations in connectivity, which ultimately result in large functional changes, occur early in sensory processing at the level of the retina or primary afferents in the somatosensory system?

Recently, we have begun a series of studies on two types of mutant mice, one lacking the $\text{Na}^+\text{-K}^+\text{-2Cl}^-$ cotransporter (NKCC1) (Flagella et al., 1999) and the other lacking the plasma membrane $\text{Ca}^{2+}\text{-ATPase}$ isoform2 (PMCA2) (Kozel et al., 1998). These mice are well suited for our study because the functional and anatomical abnormalities of the cochlea have been well characterized. NKCC1 null (NKCC1^{-/-}) and PMCA2 null (PMCA2^{-/-}) mice are congenitally deaf due to abnormalities in the morphology and function of the cochlea. These mice have a highly reduced eighth nerve, fail to develop an endocochlear potential, and have no auditory brainstem response (Kozel et al., 1998; Flagella et al., 1999). Thus, the developing nervous system of these mice never has access to sensory-driven activity from the cochlea. Studying these mice has allowed us to examine the type of compensatory anatomical changes that occur in other sensory systems, which can account for the functional changes observed in the neocortex (Hunt et al., 2002). Further, these studies have allowed us to address larger questions regarding the role of patterned activity from peripheral sensory receptor

arrays in the formation of appropriate connections in development, and the extent to which any particular pattern of connectivity that defines a given sensory system is the result of relative activity patterns between all sensory systems.

In the current study, we compared the retinofugal pathway in normal and congenitally deaf mice by making intraocular injections of neuroanatomical tracers into each eye, and relating transported tracers to architectonically defined nuclei in the thalamus and layers of the superior colliculus.

MATERIALS AND METHODS

NKCC1 and PMCA2 Knockout Mice

Both the basolateral $\text{Na}^+\text{-K}^+\text{-2Cl}^-$ cotransporter (NKCC1) and plasma membrane $\text{Ca}^{2+}\text{-ATPase}$ isoform 2 (PMCA2) knockout mice were originally analyzed on a mixed Black Swiss and 129/SvJ background (Kozel et al., 1998; Flagella et al., 1999).

NKCC1, which mediates the electroneutral transport of 1 Na^+ , 1 K^+ , and 2 Cl^- into the cell, is a member of the cation (Na^+ and/or K^+)-coupled chloride transporter family found in a large number of cell types. In the nervous system, these proteins are found in the olfactory bulb, the cerebellum, the inner ear, and transiently in the cortex and hippocampus (late embryonic to early postnatal) (Kaplan et al., 1996; Hübner et al., 2001; Kanaka et al., 2001). Despite the important role of NKCC1 in cellular ion homeostasis, NKCC1^{-/-} mice live for at least 60 weeks in the laboratory setting, well into adulthood.

Histological analysis of the inner ear of NKCC1^{-/-} mice reveals several striking abnormalities, including a collapsed Reissner's membrane and virtually no scala media lumen, accumulation of calcified material on the tectorial membrane, an absence of the tunnel of Corti (although this was not consistently observed), loss of inner and outer hair cells, a reduction of spiral ganglion cells, and abnormalities in marginal cells (Flagella et al., 1999; Pace et al., 2001). NKCC1^{-/-} mice have no endocochlear potential (Dou et al., 2000) and no auditory brainstem response (ABR) for broadband clicks or pure tone frequencies of 8–32 kHz at 20–100 db (Flagella et al., 1999). Thus, these mice are profoundly deaf.

While NKCC1 is highly expressed in only a few portions of the nervous system (Kanaka et al., 2001), the possibility that the changes in sensory system pathways that occur are the result of abnormalities of portions of the nervous system other than the inner ear cannot be completely ruled out. One way we attempted to circumvent this problem was to use two different knockouts with one major overlapping phenotypic characteristic, a morphologically aberrant and functionally inactive cochlea. We reasoned that while the loss of each particular gene may have a number of effects, similar changes in the nervous system that occur in both types of mutant mice are likely to be from cochlear dysfunction (the only common feature they share). Therefore, we also used mice lacking PMCA2 in these experiments. PMCA2 is expressed in hair bundles of cochlear hair cells (Dumont et al., 2001) and in cell bodies in the Purkinje cell and molecular layer of the cerebellum (Stauffer et al., 1997; Yamoah et al., 1998). In the inner ear, PMCA2 is involved in the extrusion of Ca^{2+} into the endolymph. PMCA2^{-/-} mice have both hearing and vestibular disorders, as well as a range of abnormalities in the organ of Corti, although not as dramatic as the

NKCC1^{-/-} mice. Auditory brainstem responses are absent in PMCA2^{-/-} mice for broadband clicks and for pure tones ranging from 8 to 32 kHz at sound pressure levels of 20–100 db (Kozel et al., 1998). These mice, like the NKCC1^{-/-} mice, are profoundly deaf.

Surgical Procedures and Injections of Neuroanatomical Tracers

Retinofugal connections were examined in four normal adult mice and six congenitally deaf (four NKCC1^{-/-} and two PMCA2^{-/-}) adult mice (3–7 months). Anesthesia was induced by placing the animals in an anesthesia chamber and administering 2.5% isoflurane. Once anesthetized, the animal was placed in a stereotaxic frame and anesthesia was delivered at 1.25–1.75% through a specially fitted cone placed over the snout. Atropine (0.06 mg/kg) and doxapram hydrochloride (1.5 mg/kg) were administered intramuscularly prior to surgery. Small subcutaneous injections of 2% lidocaine were made around the eyes. Body temperature, respiration rate, and heart rate were monitored throughout the experiment.

Intraocular injections were made with a 30 gauge needle attached to a 10 μl Hamilton syringe. The eye was gently manipulated to expose the sclera, the needle was inserted into the vitreous humor, and the tip of the syringe was visualized. Each animal received a 5 μl injection of 0.5% cholera toxin subunit B-rhodamine (BTRITC; Molecular Probes, Eugene, OR) into the right eye and a 5 μl injection of 0.5% fluorescein isothiocyanate isomer conjugate (BFITC; Molecular Probes) into the left eye. This volume of tracer has been used successfully to examine retinofugal projections in small rodents, including mice (Godement et al., 1984; Fukuda et al., 1986; Mikkelsen, 1992; Uchiumi et al., 1995). After each injection, sterile ophthalmic ointment (Neosporin) was topically applied to prevent leakage of tracer out of the eye and to prevent infection. Two days were allowed for the transport of the tracer, after which the animals were euthanized with pentobarbitone sodium (60 mg/kg) administered intraperitoneally, and transcardially perfused with 0.9% saline followed by 4% paraformaldehyde in phosphate buffer (PB; pH 7.4) and 4% paraformaldehyde with 10% sucrose in PB (pH 7.4). The brain was removed from the skull and cryoprotected overnight in 30% sucrose in PB. All brains were cut coronally at 35 μm on a freezing microtome and sections were stored in 0.1 M PB. All experimental procedures were approved by the Animal Use and Care Administrative Committee of the University of California, Davis, and conformed to NIH guidelines.

Tissue Preparation

For all cases, alternate sections were mounted for fluorescence microscopy or stained for Nissl substance. In two cases (02-113 and 03-10), an extra series was processed for cytochrome oxidase (CO) (Carroll and Wong Riley, 1984), and in one case (03-120), an extra series was processed for myelin (Gallyas, 1979).

To verify injection sites, the eyes were removed from the orbit, the retinas were dissected from the sclera and pigment epithelium and flattened using four radial cuts. The flattened retina was mounted for fluorescence microscopy. Two retinæ, which did not receive injections, were flat-mounted and prepared for fluorescence microscopy. These served as controls for our injected retinæ.

TABLE 1. Neuroanatomical abbreviations

Abbreviation	Area
3N	oculomotor nucleus
A	responds to auditory stimuli
A1	Primary auditory cortex
APT	Anterior pretectal nucleus
Aud	Auditory belt
BIC	nucleus of the brachium of the inferior colliculus
Bic	brachium of the inferior colliculus
Cp	Cerebral peduncle
Csc	commissure of the superior colliculus
CT	caudotemporal area
Deep SC	deep superior colliculus
DpG	deep gray layer of superior colliculus
DpWh	deep white layer of superior colliculus
ECIC	External cortex of the inferior colliculus
IGL	intergeniculate leaflet
InG	intermediate gray layer of the superior colliculus
InWh	intermediate white layer of the superior colliculus
LGd	lateral geniculate nucleus, dorsal part
LGv	lateral geniculate nucleus, ventral part
LGvl	lateral geniculate nucleus, ventral, lateral
LGvm	lateral geniculate nucleus, ventral, medial
LP	lateral posterior nucleus
MGd	medial geniculate nucleus, dorsal division
MGm	medial geniculate nucleus, magnocellular division
MGN	medial geniculate nucleus, ventral division
MGv	medial geniculate nucleus, ventral division
MHb	medial habenular nucleus
MM	medial mammillary nucleus, medial part
MT	medial terminal nucleus
Op	optic nerve layer of the superior colliculus
opt	optic tract
PAG	periaqueductal grey
Pf	parafascicular thalamic nucleus
PIL	posterior intralaminar thalamic nucleus
PP	peripeduncular nucleus
PT	pretectal nucleus
S	responds to somatic stimuli
S1	primary somatosensory cortex
SC	superior colliculus
SNR	substantia nigra, reticular part
STh	subthalamic nucleus
SuG	superficial gray layer of the superior colliculus
V	responds to visual stimuli
V1	primary visual cortex
VP	ventral posterior nucleus
Vpl	ventral posterolateral thalamic nucleus
VPm	ventral posteromedial thalamic nucleus
ZI	zona incerta
ZID	zona incerta, dorsal part
ZIV	zona incerta, ventral part

Data Analysis

Anterogradely labeled axon terminals and portions of axons were plotted using a Nikon E400 fluorescence mi-

croscope attached to an Accustage MD3 Digitizer and MD Plot software (Accustage, Shoreview, MN). All plotted sections included the entire outline of the section, blood vessels, and tissue artifacts. These types of reconstructions were made of every other section mounted for fluorescence microscopy throughout the entire midbrain and dorsal thalamus. Similar reconstructions were made of the flat-mounted retinae. Architectonic boundaries of midbrain and thalamic structures were made by aligning blood vessels, tissue outlines, and other tissue artifacts of adjacent Nissl-, CO-, or myelin-stained sections using a camera lucida attached to a Zeiss Stemi SV6 stereoscope. Comprehensive reconstructions were scanned using HP Scanjet 6300 Scanner and Software (HP, Palo Alto, CA), and illustrations were created using Canvas 9.0 (Deneba, British Columbia, Canada). Digital photomicrographs were taken with a Spot RT Slider digital camera and Spot camera software (Diagnostic Instruments, Sterling Heights, MI), and Adobe Photoshop 7.0 (Adobe, San Jose, CA) was used to adjust contrast and brightness of digital photomicrographs so that they most closely resembled the actual tissue.

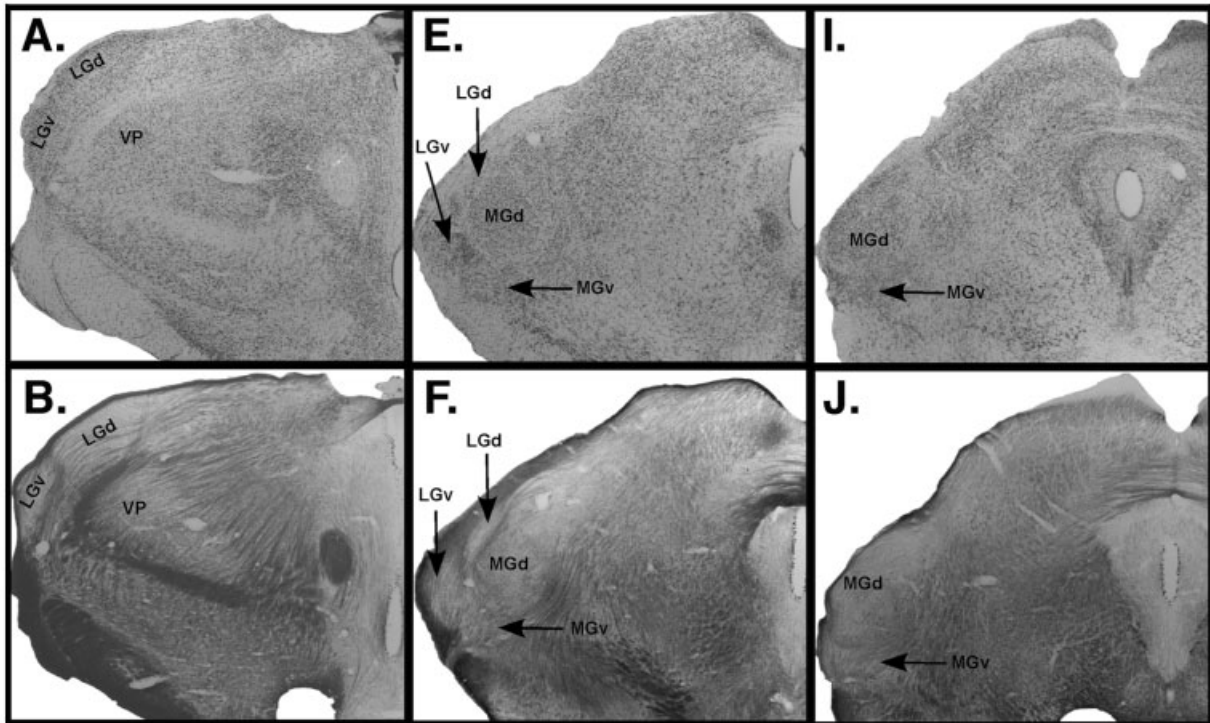
RESULTS

Injection Sites and Uptake Zones

In all cases in which the retina was dissected and reconstructed, several features were noted. The first was a very brightly fluorescing region, which marked the location of the Hamilton syringe entry and the largest deposit of the tracer. The second feature was a lighter homogeneous fluorescence throughout the retina. This marked the uptake zone of the injection. The third feature was individually fluorescing cells indicative of local retinal connections from the core of the injection. Finally, labeled ganglion cell axons were observed traversing the retina and exiting through the optic disk. All of these features were observed for both the BTRITC and BFITC injections and in both normal and mutant animals. None of these features were observed in control retinas that did not receive an injection of a neuroanatomical tracer.

Fig. 2. The architectonic boundaries of different nuclei in the thalamus of wild-type mice (case 03-120; top two rows) and PMCA2^{-/-} mice (02-113; bottom two rows) revealed with Nissl stains (row 1 and row 3), myelin stains (row 2), and cytochrome oxidase (row 4). Rostral through caudal levels of the thalamus are viewed from left to right. At rostral levels of the thalamus (A–D), the VP, LGd, and LGv are readily distinguished in all stains in both normal (A and B) and PMCA2^{-/-} (C and D) mice. In Nissl-stained sections, these nuclei are darkly staining and densely packed. In CO-stained tissue, these nuclei are darkly stained, and in myelin stains they appear light. At more caudal levels of the thalamus (E–H), LGd and LGv appear as small wedges at the lateral aspect of the thalamus, and portions of the MGd and MGv are visible. MGd contains moderately packed, darkly stained nuclei and stains darkly for CO and lightly for myelin. MGv contains more densely packed cells that stain lightly for myelin. At far caudal levels of the thalamus (I–L), the divisions of the lateral geniculate nucleus are no longer visible, and only divisions of the medial geniculate nucleus are present. The boundaries of nuclei were derived from a combination of references on rodent thalamus, including Jones (1985), Krubitzer and Kaas (1987), Paxinos and Franklin (2001), and Paxinos and Watson (1998). Medial is to the right and dorsal is to the top. Scale bar = 1 mm.

03-120
PMCA2 +/+



02-113
PMCA2 -/-

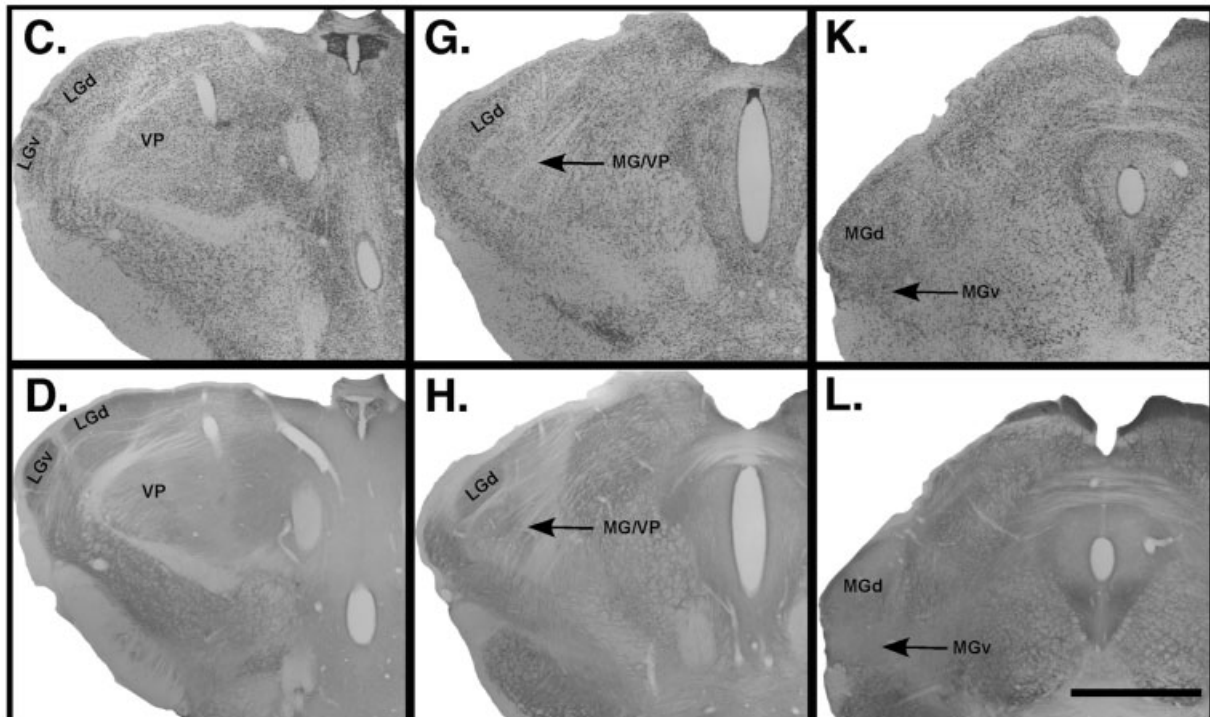


Figure 2.

Cytoarchitecture, Myeloarchitecture, and Chemoarchitecture of the Dorsal Thalamus and Superior Colliculus

The architectonic appearance of thalamic nuclei and lamina of the superior colliculus have been described for a number of rodents, including the mouse (Paxinos and Franklin, 2001), rat (Jones, 1985; Paxinos and Watson, 1998), and squirrels (Krubitzer and Kaas, 1987). In normal and mutant mice, nuclei such as the dorsal and ventral lateral geniculate nucleus (LGd and LGv, respectively; see Table 1) are well differentiated using Nissl stains. These nuclei contained moderately stained, densely clustered cells and were bounded laterally by the optic tract and were separated from each other by the cell-sparse intergeniculate leaflet (Fig. 2A and C). In sections stained for cytochrome oxidase, these nuclei are dark and homogeneously stained (Fig. 2D). In sections stained for myelin, both the LGd and LGv were very lightly stained and were surrounded by myelin-dense axons (Fig. 2B). No apparent lamina was visible in the LGd with any of the stains utilized. Posterior to the LGd and LGv is the medial geniculate complex, which is composed of three major divisions: the dorsal, ventral, and magnocellular nuclei (MGd, MGv, and MGm, respectively). In normal and mutant mice, MGd was composed of moderately sized cells and at caudal levels, resided at the lateral edge of the thalamus (Figs. 2I and K and 3B, D, and F), just ventral to the pretectum. MGv contained darker, more densely packed cells (Figs. 2I and K and 3B, D, and F), while MGm contained larger and more loosely packed cells and was located just medial to MGd and MGv. MGd and MGv stained moderately and homogeneously for CO (Fig. 2H and L), and very lightly for myelin (Fig. 2F and J). It was difficult to distinguish MGm with these stains. MG appeared to be somewhat larger in normal mice compared to both strains of mutant mice (compare Fig. 3B and D with F), but we did not attempt to quantify this difference.

The superior colliculus is composed of a number of layers, which can be distinguished using Nissl, CO, and myelin stains. The SC is traditionally divided into superficial, intermediate, and deep layers, and we have used this terminology. In both normal and deaf mice, the superficial layers of the SC contained a cell-sparse zonal layer (ZO), a cell-dense superficial gray layer (SuG), and a lightly stained optical layer (Op; Fig. 6D). SuG stained darkly for CO, and Op was lightly stained for CO (Fig. 6B). The intermediate gray layer (InG) was cell-dense, stained moderately for CO (Fig. 6), and lightly for myelin. The intermediate white layer (InWh) was cell-sparse, myelin-dense, and stained lightly and less homogeneously for CO (Fig. 6B). The deep layers consist of a moderately packed gray layer (DpG) that stained darkly for CO, and cell-sparse, myelin-dense white layer (DpWh) that stained lightly for CO.

Retinal Projections to the Dorsal Thalamus in Normal Mice

Bilateral retinal injections were made in four normal adult animals for a total of eight injections. Examination of the retinae revealed that in all cases, the injection site comprised much of the retina. Six of these injections resulted in anterogradely transported tracer in contralateral and ipsilateral midbrain structures and thalamic nuclei. In all cases in which transported tracer was observed,

labeled axon terminals were found bilaterally in the LGd and LGv. The LGd contralateral to the injected eye was almost completely filled with labeled axon terminals (Fig. 4, middle column) and contained a very small central region that was devoid of label. For all six injections, the LGd ipsilateral to the injection site contained a small, tightly packed cluster of axon terminals. In cases in which transported tracer from both the left and right eye was observed in a single section (e.g., 02-24; Fig. 4), it was found that the ipsilateral and contralateral eye input to the LGd formed a complementary, nonoverlapping pattern that has been described in a number of other rodents (Mikkelsen, 1992).

Labeled axon terminals were also observed in the ipsilateral and contralateral LGv. As with the LGd, the contralateral LGv contained labeled axon terminals that almost completely filled this nucleus (Fig. 4, middle column). However, there were a few small unlabeled portions of LGv. Ipsilateral label in LGv was sparse and formed one or several small islands. In the cases in which injections from both eyes resulted in transported tracer, it was observed that the contralateral and ipsilateral label in LGv formed complementary patterns, as with the LGd (Fig. 4, middle column).

Labeled axon terminals were observed in the contralateral intergeniculate leaflet (IGL) in all cases in which transported tracer was observed, and for two injections, in the ipsilateral IGL as well. The labeled terminals from the contralateral injection were dense and in most cases did not completely fill the nucleus. Labeled terminals resulting from the ipsilateral eye injection were sparse and formed several small islands.

Retinal Projections to the Dorsal Thalamus in $NKCC1^{-/-}$ and $PMCA2^{-/-}$ Mice

Four adult $NKCC1^{-/-}$ mice and two adult $PMCA2^{-/-}$ mice received bilateral eye injections of neuroanatomical tracers. Ten of the 12 injections resulted in transported tracer in the thalamus and midbrain. As with normal animals, dense label was observed in the contralateral LGd, and in most animals, the labeled axon terminals almost completely filled the nucleus (Fig. 4, left and right columns). We observed a small terminal free zone within the LGd in all cases, as in normal animals. Ipsilateral label in the LGd for all cases in which transported tracer was observed was very sparse and formed a small island of terminal label. When direct comparisons were made of projection patterns of both eyes, it was found that, as in normal animals, the ipsilateral and contralateral patterns of terminal label were complementary (Fig. 4, right column). Terminal label in the LGv was similar to that described in normal animals in that projections from the contralateral eye were extremely dense and almost completely filled the nucleus. Ipsilateral terminal label was sparse and formed a complementary pattern to the contralateral label. Finally, the IGL received both ipsilateral and contralateral input that was patchy and partially overlapping in all cases (Fig. 4).

Aberrant retinal projections to the dorsal thalamus were observed in both mutants. In both the $PMCA2^{-/-}$ and $NKCC1^{-/-}$ mice, densely packed terminal labeling was observed in the contralateral MGv for all injections (Figs. 3A and C and 5, left and right column). Terminal

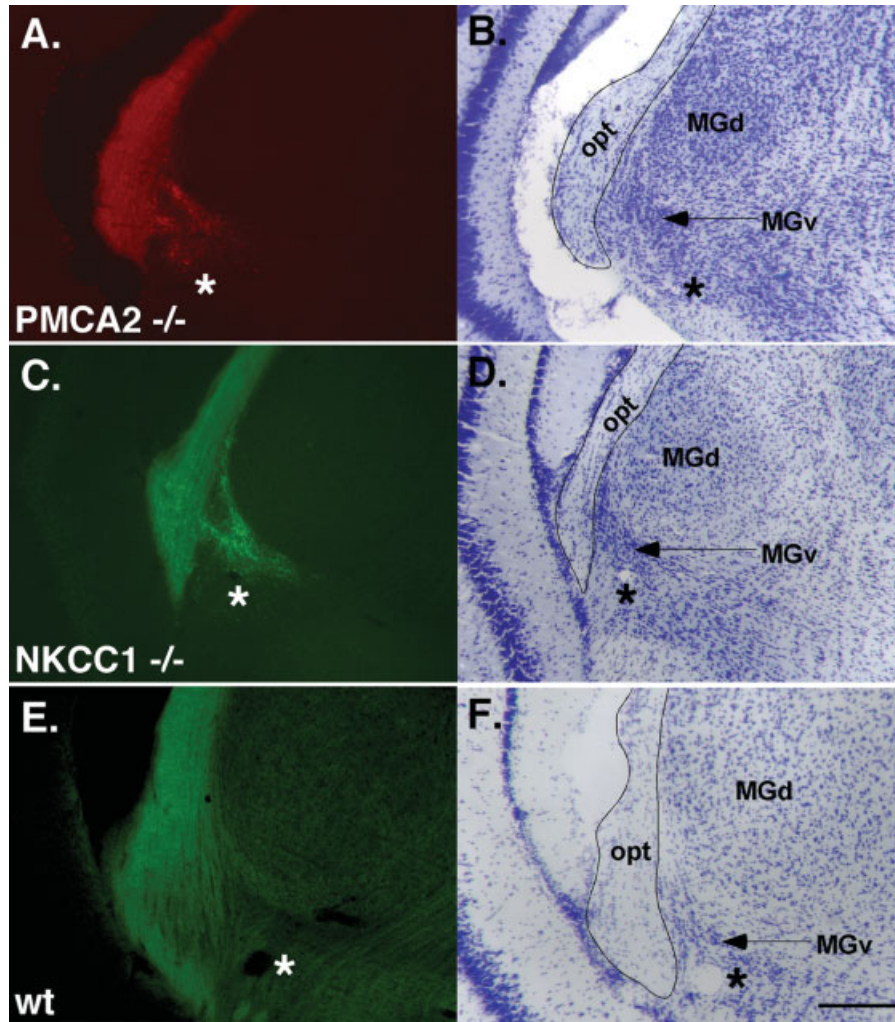


Fig. 3. Dark-field digital images of labeled terminals (left) and light-field digital images of adjacent Nissl-stained sections (right) through the dorsal thalamus at the level of the medial geniculate nucleus. In both $PMCA2^{-/-}$ mice (A and B) and $NKCC1^{-/-}$ mice (C and D), terminal

labeling is observed just medial to the optic tract (OT) in MGd and MGv. While axons in the optic tract can be readily identified, no terminal label in MG is observed in wild-type mice (E and F).

label in MGv formed patches of dark and light islands (Figs. 3 and 5). Labeled terminals were also observed in the contralateral MGd for 8 of the 10 injections (Fig. 5). Labeled terminals here were less abundant and were observed in the lateral portion of the nucleus. Four of the 10 injections resulted in label in the ipsilateral MGd and 2 of the 10 injections resulted in ipsilateral label in the MGv. In normal mice, no projections to the medial geniculate nucleus were observed (Figs. 3E and F and 5, middle column).

Retinal Projections to the Superior Colliculus in Normal Mice and Mutant Mice

Injections in both normal and mutant mice resulted in dense labeled terminals in the superficial layers of the contralateral SC, which include the SuG and the Op (Fig. 7, middle column). Terminal label was most dense in the SuG and moderately dense in the Op and was mostly

confined to the dorsal portion of Op. SuG and Op contained labeled terminals throughout their rostrocaudal extent and, in all but one case, label was homogeneous throughout its extent. In all cases in which transported tracer was observed, small, punctate patches of labeled terminals were observed in the ipsilateral superior colliculus. In both normal and mutant mice, the ipsilateral projection was in Op (Fig. 7, middle column).

Aberrant projections were observed in the contralateral superior colliculus for all injections in mutant mice in which transported tracer was observed (Figs. 6 and 7). At the rostral portion of the SC, at the juncture between the SC and the pretectum, small, punctate patches of labeled terminals were observed throughout the mediolateral extent of the intermediate gray layer (Figs. 6C and 7, left and right column). The patchy label identified in InG on first inspection looks like it could be assigned to the pretectal nucleus. However, this label is

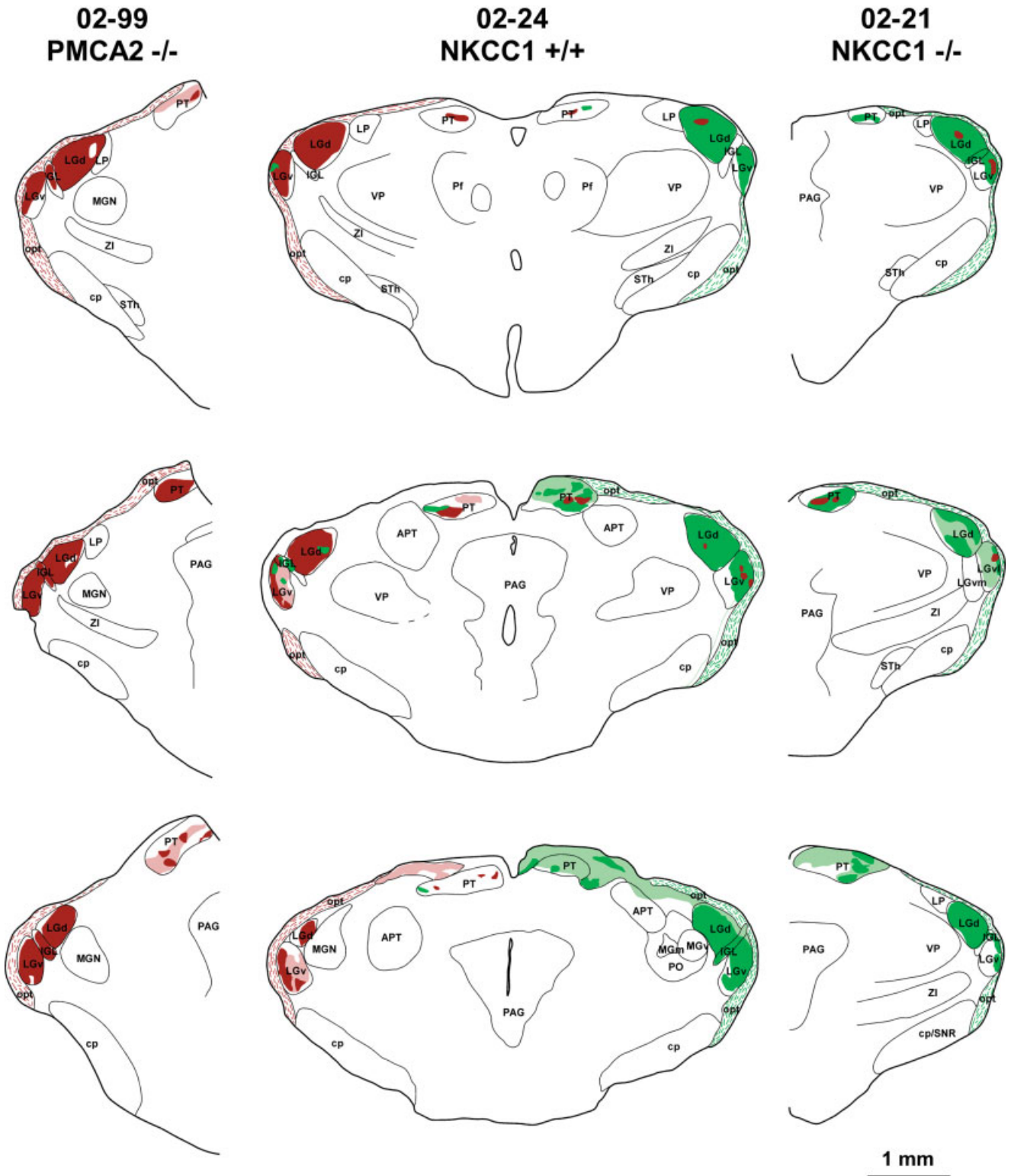


Fig. 4. Reconstructions from rostral (top row) through caudal (bottom row) levels of the thalamus of sections containing labeled axon terminals (shades of green and red) and fibers of passage (green or red small lines) following intraocular injections. Although the planes of section are not identical in these three cases, particularly for case 02-99 in which the dorsal/ventral plane is not matched to the other cases, the region of interest, the LGd and LGv of the thalamus are at approximately the same level. In normal mice (middle column), BFITC (green) was injected into the left eye and BTRITC (red) into the right eye. In *PMCA2*^{-/-} mice (left

column), BTRITC was injected into the right eye, and in *NKCC1*^{-/-} (right column) BFITC was injected into the left eye and BTRITC was injected into the right eye. Many of the patterns of contralateral and ipsilateral terminal label are strikingly similar for the LGd, LGv, IGL, and PT in both normal and the congenitally deaf mouse. Solid lines mark architectonic boundaries. Dark green and dark red mark densely labeled terminal fields and light green and red mark moderately labeled terminal fields. Red and green lines in the optic tract mark labeled axons. Dorsal is to the top and lateral is to the right and left of each section. Scale bar = 1 mm.

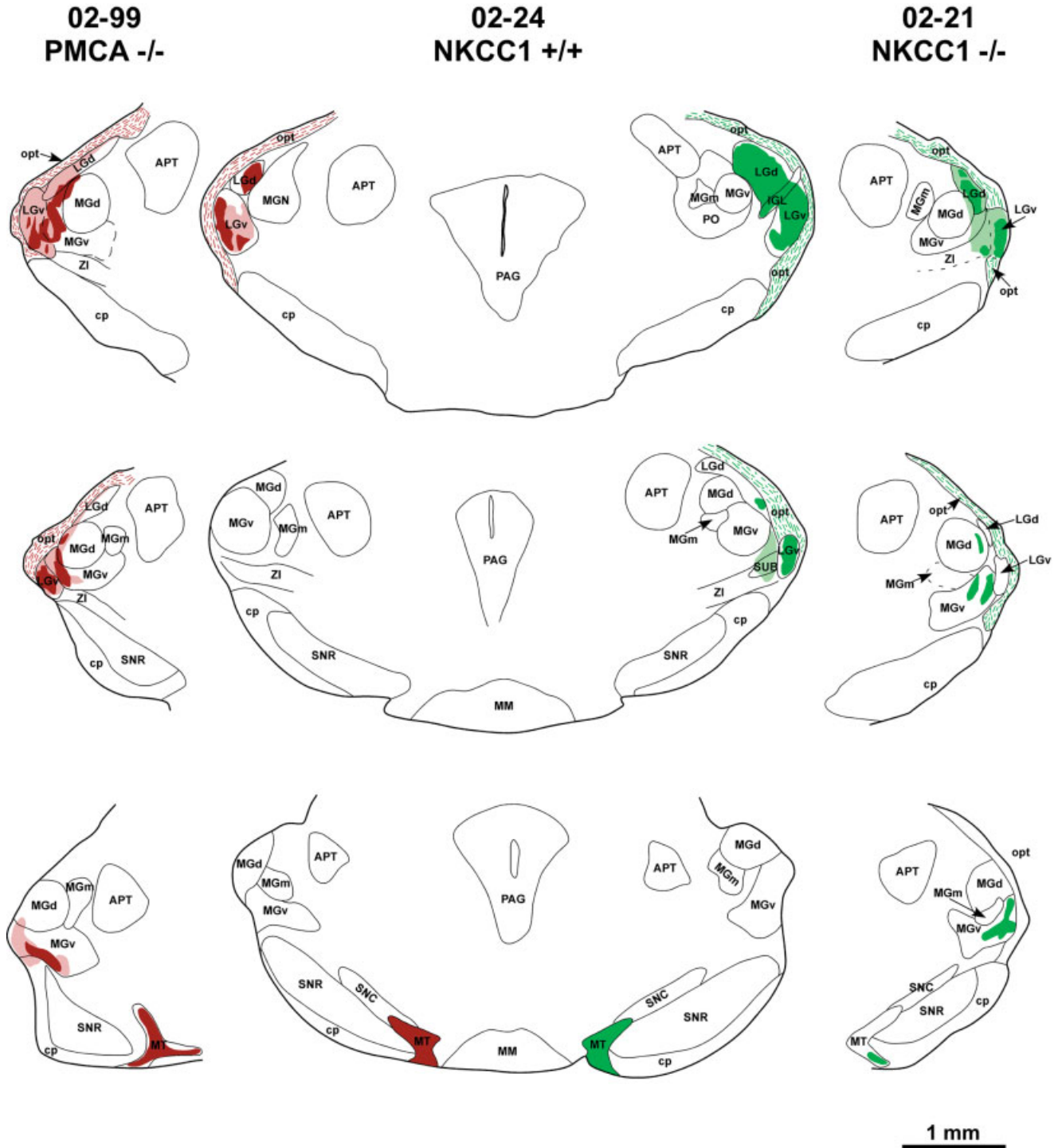


Fig. 5. Reconstructions from rostral (top) through caudal (bottom) levels of the thalamus of sections containing labeled axon terminals and labeled axons following intraocular injections in a normal mouse (middle column), a *PMCA2*^{-/-} mouse (left column), and an *NKCC1*^{-/-} mouse (right column). In the *PMCA2*^{-/-} mouse, an injection of BTRITC (red) was made in the right eye; in the normal mouse, BFITC (green) was injected in the left eye and BTRITC was injected in the right eye. In the *NKCC1*^{-/-} mouse, BFITC was injected into the left eye. Dark green and dark red marks densely labeled terminal fields and light green and red mark moderately labeled terminal fields. At rostral levels of the thalamus (top row), labeled terminals in both normal and deaf mice are observed in the LGd and LGv. At a more caudal levels, at the transition between the

lateral geniculate nucleus and the medial geniculate nucleus, the LGd and LGv can be readily identified as two small wedge-shaped structures at the lateral edge of the thalamus, and MGd and MGv are just medial to these nuclei. In both *NKCC1*^{-/-} and *PMCA2*^{-/-}, dense patches of terminal label are observed in MGd and MGv. At a more caudal levels of the thalamus (bottom row), the divisions of the lateral geniculate nucleus are no longer present. Labeled axon terminals are observed in MGv in deaf mice, but not in normal mice. In both normal and deaf mice, dense terminal label is observed in the medial terminal nucleus. Dorsal is to the top and lateral is to the right and left of each section. Labeled axons in the optic tract are marked as small lines. Scale bar = 1 mm. Other conventions as in previous figures.

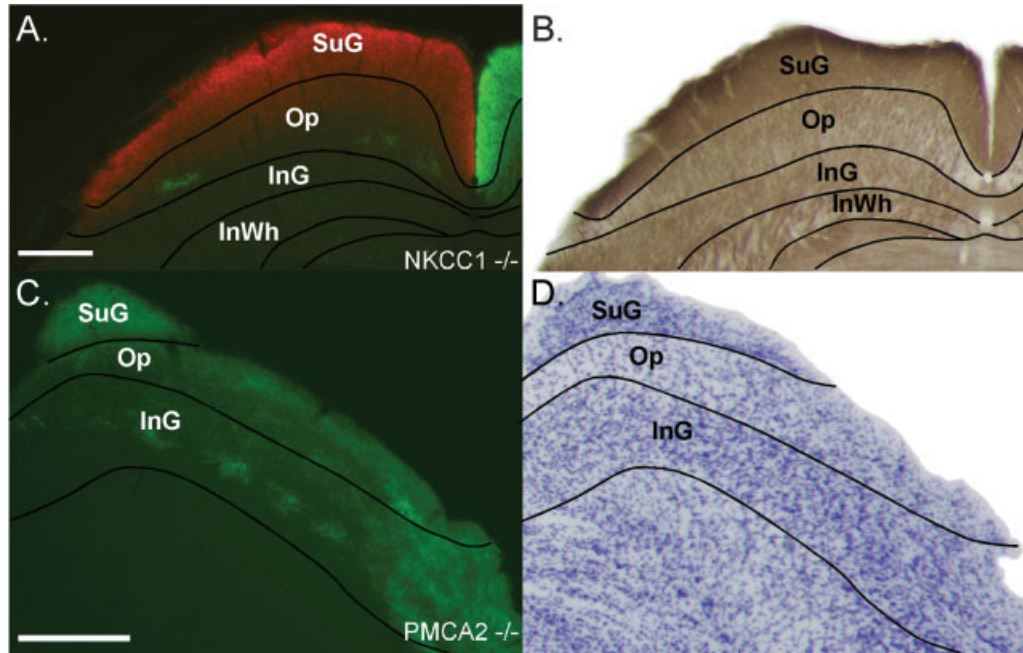


Fig. 6. Digital images of terminal labeling in the superior colliculus following injections of BTRITC (red) into the right eye and BFTIC (green) into the left eye of $NKCC1^{-/-}$ (A) and BFTIC into the left eye of $PMCA2^{-/-}$ (C) mice, both of which are congenitally deaf. Adjacent sections stained for Nissl (B) or cytochrome oxidase (D) were matched to the tissue reconstructed for labeled terminals so that architectonic boundaries could be directly related to layers in the superior colliculus. Patterns of label resulting from the eye injections were similar to that of

normal animals in that the superficial layers of the SC contained labeled terminals. Further, small patches label from the BFTIC (green) injection into the ipsilateral eye are observed in the Op (A). Aberrant projections are observed in the intermediate gray layers of the SC (C) of deaf mice. This terminal labeling forms dense patches throughout the lateral to medial extent of the nucleus. Lines in the dark-field digital images mark architectonic boundaries drawn from adjacent Nissl- and CO-stained sections. Scale bars = 250 μm . Conventions as in previous figures.

located caudal of this nucleus, and examination of adjacent Nissl-stained sections indicate that it is indeed in the InG. Throughout the rostral to middle extent of the SC, terminal label filled the Op and extended into the InG in all mutant mouse cases (Fig. 7). This was not observed in normal mice.

Other Retinal Projections in Normal and Mutant Mice

For all injections in both normal and mutant mice, terminal labeling was observed in the contralateral pretectum (Fig. 4). Label formed very dense clusters surrounded by more moderate labeling. Likewise, for all cases, labeled terminals were observed in the ipsilateral pretectum. Terminal labeling in the ipsilateral pretectum was much less extensive and formed small patches. Finally, for all injections in both normal and mutant mice, dense terminal labeling was observed in the contralateral medial terminal nucleus (MT; Fig. 5, bottom row).

DISCUSSION

We examined the retinal projections to the dorsal thalamus and midbrain structures in normal and two strains of congenitally deaf mice. The data demonstrate that while most of the projections are similar in all three groups, congenitally deaf mice have two alterations in their retinal connections. The most notable alteration is a projection to the ventral and dorsal division of the contralateral medial geniculate nucleus of the thalamus (Fig.

8). The second aberrant projection observed was with the intermediate layers of the contralateral superior colliculus (Fig. 8). In the following sections, we provide an overview of what is known about the normal projections of the eye in rodents and discuss the implications of our results for appropriate targeting of sensory system-specific connections, which we term “sensoritopic matching.”

Retinofugal Projections in Rodents

Retinal projections have been examined in a wide variety of rodents including mice (Mikkelsen, 1992), rats (Lund et al., 1974; Reese and Cowey, 1983, 1987; Mikkelsen, 1992), ground squirrels (Kicliter and Bruce, 1983; Petry et al., 1989; Lugo and Kicliter, 1995; Major et al., 2003), eastern gray squirrels (Cusick and Kaas, 1982), chipmunks (Fukuda et al., 1986), gerbils (Mikkelsen, 1992; Fite et al., 2003), moles (Herbin et al., 1994), hamsters (Crain and Hall, 1980; Mikkelsen, 1992; Ling et al., 1998), guinea pigs (Lazar, 1983), and voles (Uchiumi et al., 1995). The present investigation of retinal projections is consistent with all previous studies in rodents (except the blind mole rat) in that all species have dense contralateral projections to the LGd, LGv, and IGL of the dorsal thalamus, and to the superficial layers of the superior colliculus. Similarly, all rodents have ipsilateral projections to the LGd, LGv, IGL, and the optical layer of the superior colliculus.

An important and consistent observation in all studies of retinofugal projections in rodents is that no con-

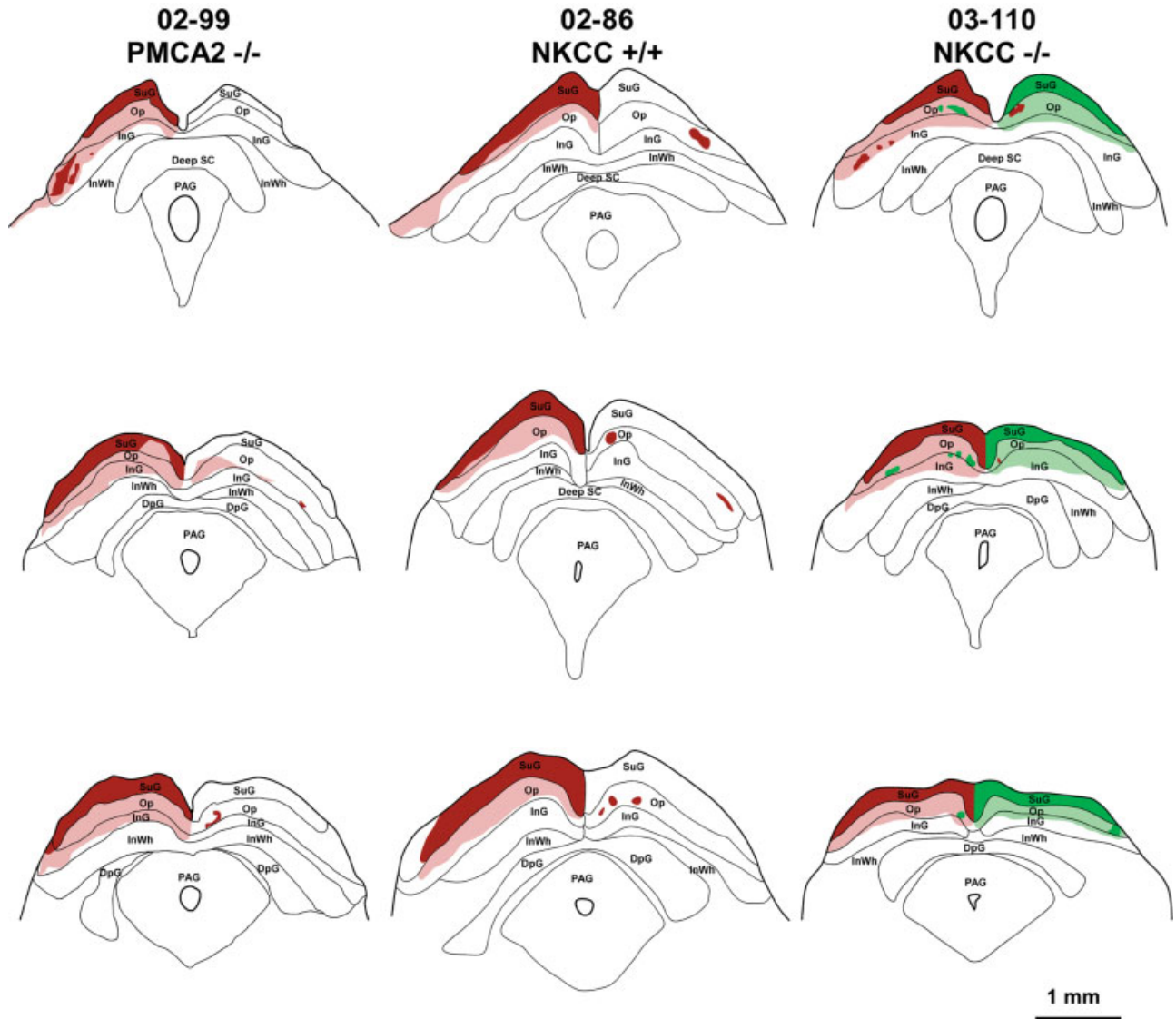


Fig. 7. Reconstructions from rostral (top) through caudal (bottom) levels of the superior colliculus of sections containing labeled axon terminals following injections of BTRITC (red) into the right eye of a normal mouse (middle column), BTRITC into the right eye of a $PMCA2^{-/-}$ mouse (left column), and BTRITC into the right eye and a BFTIC (green) into the left eye of an $NKCC1^{-/-}$ mouse. Patterns of contralateral and ipsilateral label are similar in normal and deaf mice in that terminal label is observed in the superficial layers of the contralateral

superior colliculus (SuG and Op) and ipsilaterally in Op. Contralateral label was most dense in SuG and moderately dense in Op. In both layers, terminal label is evenly distributed. Ipsilaterally labeled terminals in normal and deaf mice form small patches in Op. In the congenitally deaf mice, terminal label spreads more ventrally in the superior colliculus into the intermediate gray layers (InG) of the contralateral superior colliculus. Conventions as in previous figures.

nections were found with the medial geniculate nucleus or with the intermediate layers of the contralateral superior colliculus. Divisions of the medial geniculate nucleus receive input predominantly from the central nucleus of the inferior colliculus, which is a major target of most auditory brainstem nuclei (Beyerl, 1978; Norden et al., 1983; Coleman and Clerici, 1987; Malmierca et al., 2002; Winer et al., 2002). The intermediate layers of the superior colliculus receive input from auditory cortex (Budinger et al., 2000), and subcortical structures such as the nucleus of the brachium of the inferior colliculus, the external nucleus of the inferior colliculus,

and nuclei of the lateral lemniscus (Edwards et al., 1979; Druga and Syka, 1984; Cadusseau and Roger, 1985; King et al., 1998), and contain neurons that respond to auditory stimulation (Drager and Hubel, 1975; Middlebrooks and Knudsen, 1984; Hirsch et al., 1985; King and Hutchings, 1987; Gaese and Johnen, 2000; for review, see King, 1999). Thus, the aberrant projections of the retina in our mutant mice were to subcortical auditory structures, which ultimately project to and receive projections from auditory cortex. This suggests that compensatory adaptation due to loss of sensory-driven activity from any one sensory system occurs at

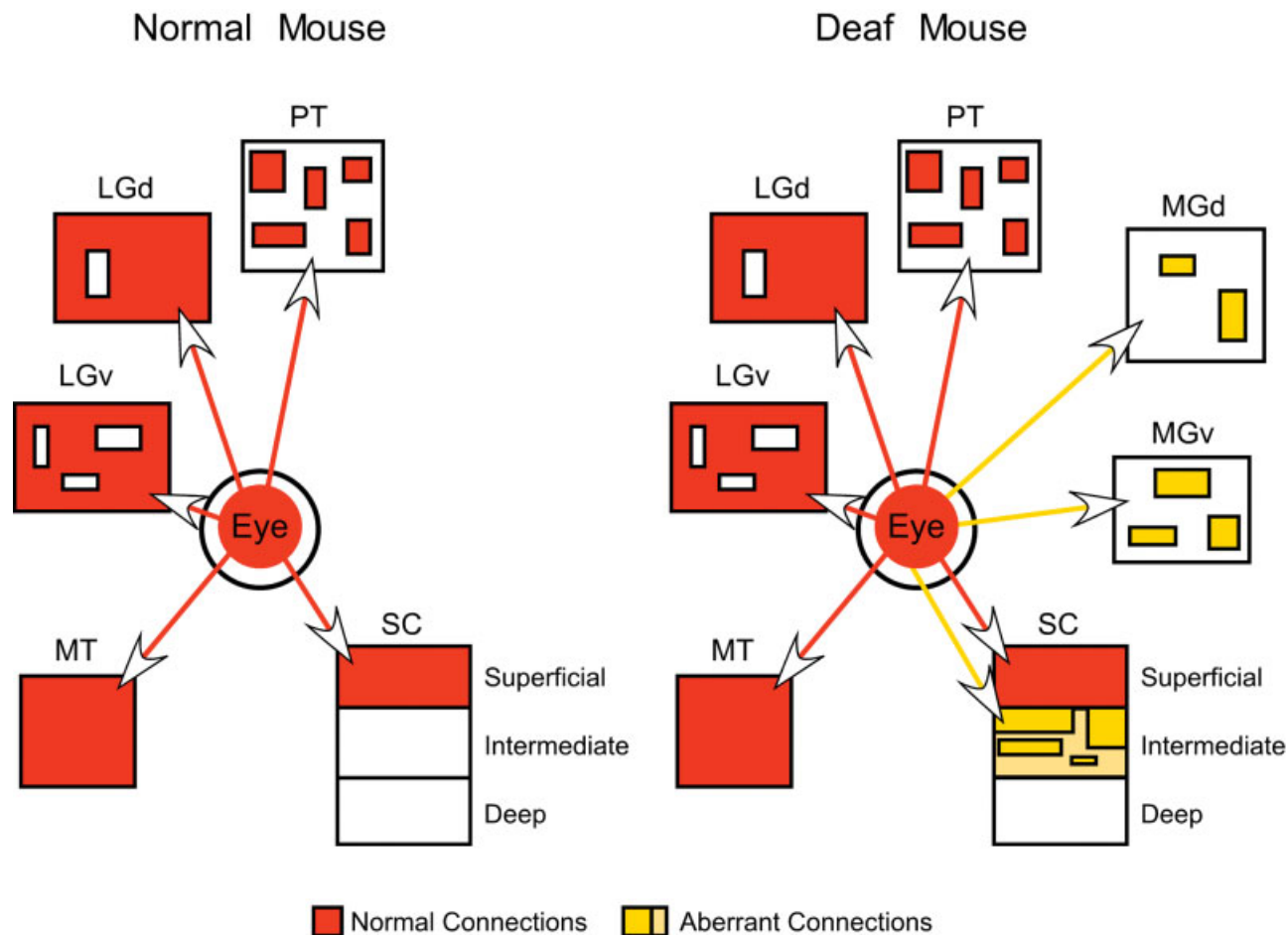


Fig. 8. Summary of contralateral retinal projections in the normal (left) and congenitally deaf (right) mouse. Most of the patterns of connections in normal and congenitally deaf mice are similar in that dense connections are observed with the contralateral LGd, LGv, IGL, PT, MT, and

superficial layers of the SC (red). Aberrant connections (yellow) are observed with the MGd, MGv, and intermediate gray layers of the SC. These nuclei of the thalamus and layers of the SC are normally associated with processing auditory inputs. Conventions as in previous figures.

very early stages of sensory processing and has a cascade of effects at all stages of processing, including the neocortex.

It should be noted that aberrant retinal projections to the medial geniculate nucleus have been surgically induced in both hamsters and ferrets by lesioning central structures such as V1, the superior colliculus, and/or the brachium of the inferior colliculus in developing animals (Schneider, 1973; Kalil and Schneider, 1975; Frost, 1981, 1986; Sur et al., 1988; Roe et al., 1993; Pallas et al., 1994). Interestingly, these latter authors conclude that the modality of a sensory thalamic nucleus is determined by its inputs during development (Sur et al., 1988). However, this model is different in two respects from the mouse models used in the current study. The first difference is that the aberrant projections observed in the present investigation are the consequence of alterations in sensory-driven activity from the cochlea, rather than the removal of two major targets of the retina, the superior colliculus and the LGN (via retrograde degeneration from V1 lesions) or removal of a brainstem source of auditory afferents, the brachium of the inferior colliculus. This differ-

ence is important because it distinguishes top-down rewiring, or removal of retinal targets, from bottom-up rewiring, involving the loss of auditory afferents. The second difference is that the alterations described here may be analogous to what normally occurs during evolution and may provide some insights into the developmental mechanisms, both activity-dependent and molecular, that give rise to phenotypic variability in subcortical and cortical organization in mammals. These naturally occurring developmental changes are likely to occur at multiple levels of the nervous system such that genetically mediated reduction of peripheral afferents leads to decreases in activity of the normal target. This target in turn may fail to express molecules that restrict afferent terminations. Such a series of events would allow novel pathways to form.

Relative Activity Between Sensory Systems Is Necessary for Sensoritopic Matching

The role of activity for appropriate circuit formation has been described for all levels of the nervous system (for reviews, see Katz and Shatz, 1996; Ruthazer and Cline,

2004). The visual system has traditionally been the model system for understanding the role of activity in the formation of layer-specific zones in the lateral geniculate nucleus and ocular dominance columns in the visual cortex. The consensus across studies is that retinal ganglion cell axons from each eye are initially intermixed in the LGN. Over time, retinal inputs form eye-specific domains within the LGN due to differences in spontaneous and driven activity from each eye (Shatz, 1983; Penn et al., 1998; for review, see Shatz, 1996). For ocular dominance columns in the primary visual cortex, initial afferents from the LGN are largely overlapping in layer IV, and gradually segregate into eye-specific domains during a prenatal and postnatal period, with the onset of patterned retinal activity (Hubel and Freeman, 1977; LeVay et al., 1980; for review, see Ruthazer and Cline, 2004).

While the role of both spontaneous and patterned activity in the formation of appropriate connections has been well investigated within a particular sensory system, specifically the visual system, there is little understanding of how the magnitude of activity in any one sensory system and the relative activity patterns across sensory systems contribute to the establishment of appropriate sensoritopic connections. For example, what are the mechanisms by which a particular subcortical or cortical structure assumes a unimodal or multimodal function? Comparative studies in highly derived species provide some insight into this issue. The blind mole rat is a subterranean rodent with atrophied, subcutaneous eyes, a greatly reduced optic nerve, and specialized skin (the buccal ridge), which completely covers the eyes (Klauer et al., 1997; David-Gray et al., 1998). Thus, the overall activity generated from the retina is greatly reduced compared to the activity generated from the cochlea, the somatic receptors, and the olfactory epithelium. The visual system in these animals is involved predominantly in the establishment and maintenance of circadian rhythms (Cooper et al., 1993; David-Gray et al., 1998). 2-deoxyglucose and electrophysiological recording studies in this animal demonstrate that the lateral geniculate nucleus is activated by auditory stimulation, as is the visual cortex (Bronchti et al., 1989, 2002; Heil et al., 1991; Sadka and Wollberg, 2004). Interestingly, early in development, normal retinogeniculate patterns of connectivity can be observed, but later degenerate and are absent in the adult (Bronchti et al., 1991; Cooper et al., 1993). In the absence of activity from the retina, the lateral geniculate nucleus is taken over by inputs from the inferior colliculus (Doran and Wollberg, 1994). These data indicate that with large alterations in the magnitude of activity across sensory systems, subcortical structures associated with the reduced system are taken over, at least in part, by other sensory systems, and this in turn appears to have a very large effect on the organization and function of the neocortex.

Our results of aberrant visual inputs to subcortical structures normally associated with auditory processing are analogous to the innervation of visual structures by auditory inputs in the blind mole rat. Further, recent results on the neocortex of these congenitally deaf mice indicate that massive reorganization occurs in that auditory cortex is taken over by somatic and visual inputs (Hunt et al., 2002). This result is similar to the results of functional imaging studies in congenitally deaf humans described earlier. Obviously, this functional reorganization of the neocortex is at least partly accounted for by

alterations in connections at the earliest stages of sensory processing. Given that similar types of cross-modal plasticity have been observed in congenitally deaf humans and that recent studies demonstrate that these individuals have heightened capabilities for the other senses, these aberrant connections are functionally optimized and may allow for enhanced sensory performance of remaining sensory systems.

Contribution of Activity and Molecular Cues to Sensoritopic Organization

The role of particular molecules in establishing appropriate topographic matching of connections between structures has been well studied in the visual system. For example, Eph receptors in the retina and their ephrin ligands in the superior colliculus form gradients that provide a molecular substrate for the development of topographically matched connections between these structures, which ultimately underlies functional map organization in the adult superior colliculus (Frisén et al., 1998; for reviews, see Flanagan and Vanderhaeghen, 1998; Goodhill and Richards, 1999; O'Leary and Wilkinson, 1999). Such gradient matching has only recently been established for connections between sensory receptor arrays and their thalamic counterparts. For instance, ephrin-A2 and -A5 have been demonstrated to play an important role in retinogeniculate topographic connection formation (Feldheim et al., 1998, 2000). Further, in mutant mice that lack both ephrin-A2 and ephrin-A5, surgically induced invasion of the medial geniculate nucleus by retinal ganglion cell axons is enhanced, suggesting that these proteins are involved in regulating sensoritopic mapping within the dorsal thalamus (Lyckman et al., 2001).

In addition to the gradient-matching mechanisms that are involved in setting up topographic connections within a unimodal structure, there is an abundance of data that indicate that spontaneous and patterned activity are important for map formation in the superior colliculus and laminar organization within the LGd (Shatz, 1983; Sretevan and Shatz, 1986; Grubb et al., 2003; McLaughlin et al., 2003; Schmidt, 2003; for review, see Ruthazer and Cline, 2004). Activity from developing peripheral sensory receptor arrays may regulate the expression of molecules through calcium and CRE/CREB-regulated transcriptional pathways. CRE/CREB-mediated gene expression has been demonstrated in the developing thalamus, prior to visual experience (Pham et al., 2001). Mice deficient in the CREB protein develop more diffuse, less refined ipsilateral and contralateral retinal connections with the LGd. In addition, monocular enucleation causes a down-regulation of CRE lacZ expression, indicating that activity from the peripheral receptor array normally regulates gene expression through the CRE/CREB pathway. This CRE/CREB pathway may regulate the formation of sensoritopic connections in the thalamus and midbrain structures by altering the expression patterns of molecules that have been associated with sensoritopic matching in the thalamus and midbrain, such as the ephrins, or transcription factors that have been shown to be restricted to particular thalamic nuclei, such as *Gbx2*, *Pax6*, and *Ngn2* (Nakagawa and O'Leary, 2001). Support for an ephrin-mediated regulation of unimodal connections in the midbrain is provided by Frisén et al. (1998), who demonstrate that the absence of ephrin-A5 in mice results not only in

disruption of topographic connections in the superior colliculus, but an invasion of retinal ganglion cell axons into the inferior colliculus. It is also possible that the loss of activity in the projection target, the MG, induces molecular changes in the MG and invokes sprouting of axons from adjacent pathways, such as the optic tract.

Recent evidence indicates that there are distinct patterns of expression of transcription factors (e.g., *Lhx1*, *Lhx2*, *Gbx2*, *Pax6*) in the developing thalamus associated with particular nuclei, which in combination with other molecules may be responsible for specifying nucleus-specific properties and ultimately establishing appropriate afferent and efferent connections of the thalamus (Nakagawa and O'Leary, 2001). The fact that despite congenital deafness, the MGN appears to be histologically normal and the majority of retinal ganglion cells establish appropriate connections lends support to the proposition that combinations of expression of particular genes intrinsic to the dorsal thalamus set up a basic nonvariable organization at least in terms of nuclei position and histological appearance. However, the present data suggest that activity from different sensory receptor arrays are necessary for appropriate sensoritopic mapping of connections of particular nuclei within the thalamus and layers within the colliculus. Thus, the ratio of activity from the different sensory systems may ultimately endow unimodality or multimodality of a particular subcortical structure. Further, preliminary studies in our laboratory (Hunt et al., 2002; Punj et al., 2002) indicate that alterations in connectivity have occurred throughout the nervous system in congenitally deaf mice. Such alterations in central nervous system connections have also been described in anophthalmic mice in which the inferior colliculus and the cuneate nucleus project to the LGN (Asanuma and Stanfield, 1990). Each particular alteration in turn changes the combination of inputs to a particular structure and the ratio of sensory-specific activity to that structure. These alterations, which begin at the very first stage of sensory processing, can have a cascade of bottom-up effects along the entire neuroaxis. Thus, the large functional changes observed in the neocortex of congenitally deaf humans, blind mole rats, and congenitally deaf mice could be solely accounted for by small alterations in connectivity at a number of subcortical structures resulting from changes in the ratio of activity from different sensory systems. It follows that phenotypic variability in cortical organization across mammals need not be mediated by genes intrinsic to the neocortex.

ACKNOWLEDGMENTS

The authors thank Sarah Karlen and Jeffery Padberg for helpful suggestions on this manuscript. Supported by the McDonnell Foundation Grant (220020053 to L.K.), the National Institute of Neurological Disorders and Stroke (NINDS) (R01-NS35103 to L.K.), and the National Institute of Deafness and Other Communications Disorders (NIDCD) (R01 DC04542 to E.N.Y.).

LITERATURE CITED

- Armstrong B, Neville HJ, Hillyard S, Mitchell T. 2002. Auditory deprivation affects processing of motion, but not color. *Brain Res Cogn Brain Res* 14:422–434.
- Asanuma C, Stanfield BB. 1990. Induction of somatic sensory inputs to the lateral geniculate nucleus in congenitally blind mice and in phenotypically normal mice. *Neuroscience* 39:533–545.
- Bavelier D, Neville HJ. 2002. Cross-modal plasticity: where and how? *Nat Rev Neurosci* 3:443–452.
- Beyerl B. 1978. Afferent projections to the central nucleus of the inferior colliculus in the rat. *Brain Res* 145:209–223.
- Bronchti G, Heil P, Scheich H, Wollberg Z. 1989. Auditory pathway and auditory activation of primary visual targets in the blind mole rat (*Spalax ehrenbergi*): I, 2-deoxyglucose study of subcortical centers. *J Comp Neurol* 284:253–274.
- Bronchti G, Rado R, Terkel J, Wollberg Z. 1991. Retinal projections in the blind mole rat: WGA-HRP tracing study of a natural degeneration. *Brain Res Dev Brain Res* 58:159–170.
- Bronchti G, Heil P, Sadka R, Hess A, Scheich H, Wollberg Z. 2002. Auditory activation of “visual” cortical areas in the blind mole rat (*Spalax ehrenbergi*). *Eur J Neurosci* 16:311–329.
- Büchel C, Price C, Frackowiak RS, Friston K. 1998. Different activation patterns in the visual cortex of late and congenitally blind subjects. *Brain* 121:409–419.
- Budinger E, Heil P, Scheich H. 2000. Functional organization of auditory cortex in the Mongolian gerbil (*Meriones unguiculatus*): IV, connections with anatomically characterized subcortical structures. *Eur J Neurosci* 12:2452–2474.
- Cadusseau J, Roger M. 1985. Afferent projections to the superior colliculus in the rat, with special attention to the deep layers. *J Hirnforsch* 26:667–681.
- Carroll EW, Wong-Riley MTT. 1984. Quantitative light and electron microscopic analysis of cytochrome oxidase-rich zones in the striate cortex of the squirrel monkey. *J Comp Neurol* 222:1–17.
- Catalan-Ahumada M, Deggouj N, De Volder A, Melin J, Michel C, Veraart C. 1993. High metabolic activity demonstrated by positron emission tomography in human auditory cortex in case of deafness of early onset. *Brain Res* 623:287–292.
- Cohen L, Celnik P, Pascual-Leone A, Corwell B, Faiz L, Dambrosia J, Honda M, Sadato N, Gerloff C, Catala D, Hallett M. 1997. Functional relevance of cross-modal plasticity in blind humans. *Nature* 389:180–183.
- Coleman JR, Clerici WJ. 1987. Sources of projections to subdivisions of the inferior colliculus in the rat. *J Comp Neurol* 262:215–226.
- Cooper HM, Herbin M, Nevo E. 1993. Visual system of a naturally microphthalmic mammal: the blind mole rat, *Spalax ehrenbergi*. *J Comp Neurol* 328:313–350.
- Crain B, Hall W. 1980. The organization of afferents to the lateral posterior nucleus in the golden hamster after different combinations of neonatal lesions. *J Comp Neurol* 193:403–412.
- Cusick C, Kaas J. 1982. Retinal projections in adult and newborn grey squirrels. *Dev Brain Res* 4:275–284.
- David-Gray Z, Janssen J, DeGrip W, Nevo E, Foster R. 1998. Light detection in a “blind” mammal. *Nat Neurosci* 1:655–656.
- Doron N, Wollberg Z. 1994. Cross-modal neuroplasticity in the blind mole rat *Spalax ehrenbergi*: a WGA-HRP tracing study. *Neuroreport* 5:2697–2701.
- Dou H, Jimenez A, Flagella M, Lonsbury-Martin B, Erway L, Cardell E, Shull GE, Yamoah E. 2000. The functional roles of Na-K-2Cl cotransporter in age-related hearing loss. *Soc Neurosci Abstr* 26:826–810.
- Drager U, Hubel D. 1975. Responses to visual stimulation and relationship between visual, auditory, and somatosensory inputs in mouse superior colliculus. *J Neurophysiol* 38:690–713.
- Druga R, Syka J. 1984. Projections from auditory structures to the superior colliculus in the rat. *Neurosci Lett* 45:247–252.
- Dumont RA, Lins U, Filoteo AG, Penniston JT, Kachar B, Gillespie PG. 2001. Plasma membrane Ca²⁺-ATPase isoform 2a is the PMCA of hair bundles. *J Neurosci* 21:5066–5078.
- Edwards S, Ginsburgh C, Henkel C, Stein B. 1979. Sources of subcortical projections to the superior colliculus in the cat. *J Comp Neurol* 184:309–329.
- Feldheim DA, Vanderhaeghen P, Hansen MJ, Frisén J, Lu Q, Barbacid M, Flanagan JG. 1998. Topographic guidance labels in a sensory projection to the forebrain. *Neuron* 21:1303–1313.
- Feldheim DA, Kim YI, Bergemann A, Frisén J, Barbacid M, Flanagan J. 2000. Genetic analysis of ephrin-A2 and ephrin-A5 shows their requirement in multiple aspects of retinocollicular mapping. *Neuron* 25:563–574.

- Finney E, Fine I, Dobkins K. 2001. Visual stimuli activate auditory cortex in the deaf. *Nat Neurosci* 4:1171–1173.
- Fite K, Birkett M, Smith A, Janusonis S, McLaughlin S. 2003. Retinal ganglion cells projecting to the dorsal raphe and lateral geniculate complex in Mongolian gerbils. *Brain Res* 973:146–150.
- Flagella M, Clarke LL, Miller ML, Erway LC, Giannella RA, Andringa A, Gawenis LR, Kramer J, Duffy JJ, Doetschman T, Lorenz JN, Yamoah EN, Cardell EL, Shull GE. 1999. Mice lacking the basolateral Na-K-2Cl cotransporter have impaired epithelial chloride secretion and are profoundly deaf. *J Biol Chem* 274:26946–26955.
- Flanagan J, Vanderhaeghen P. 1998. The ephrins and eph receptors in neural development. *Annu Rev Neurosci* 21:309–345.
- Frisén J, Yate PA, McLaughlin T, Friedman GC, O'Leary DDM, Barbacid M. 1998. Ephrin-A5 (AL-1/RAGS) is essential for proper retinal axon guidance and topographical mapping in the mammalian visual system. *Neuron* 20:235–243.
- Frost DO. 1981. Orderly Anomalous retinal projections to the medial geniculate, ventrobasal, and lateral posterior nuclei of the hamster. *J Comp Neurol* 203:227–256.
- Frost DO. 1986. Development of anomalous retinal projections to nonvisual thalamic nuclei in Syrian hamsters: a quantitative study. *J Comp Neurol* 252:95–105.
- Fukuda Y, Takatsuji K, Sawai H, Wakakuwa K, Watanabe M, Mitani-Yamanishi Y. 1986. Ipsilateral retinal projections and laminations of the dorsal lateral geniculate nucleus in the eastern chipmunk (*Tamias sibiricus asiaticus*). *Brain Res* 384:373–378.
- Gaese B, Johnen A. 2000. Coding for auditory space in the superior colliculus of the rat. *Eur J Neurosci* 12:1739–1752.
- Gallyas F. 1979. Silver staining of myelin by means of physical development. *Neurology* 1:203–209.
- Godement P, Salaun J. 1984. Origins of the ipsilateral retinal projections in prenatally-enucleated mice. *J Embryol Exp Morphol* 82:224.
- Goodhill G, Richards L. 1999. Retinotectal maps: molecules, models and misplaced data. *Trends Neurosci* 22:529–534.
- Grubb M, Rossi F, Changeux J-P, Thompson I. 2003. Abnormal functional organization in the dorsal lateral geniculate nucleus of mice lacking the B2 subunit of the nicotinic acetylcholine receptor. *Neuron* 40:1161–1172.
- Heil P, Bronchti G, Wollberg Z, Scheich H. 1991. Invasion of visual cortex by the auditory system in the naturally blind mole rat. *Neuroreport* 2:735–738.
- Herbin M, Reperant J, Cooper H. 1994. Visual system of the fossorial mole-lemmings, *Ellobiustalpinus* and *Ellobius lutescens*. *J Comp Neurol* 346:253–275.
- Hirsch J, Chan J, Yin T. 1985. Responses of neurons in the cat's superior colliculus to acoustic stimuli: I, monaural and binaural response properties. *J Neurophysiol* 53:726–758.
- Hubel DH, Freeman DC. 1977. Projection into the visual field of ocular dominance columns in macaque monkey. *Brain Res* 122:336–343.
- Hübner CA, Lorke DE, Hermans-Borgmeyer I. 2001. Expression of the Na-K-2Cl-cotransporter NKCC1 during mouse development. *Mech Dev* 102:267–269.
- Hunt DL, Litinas E, Krubitzer L, Yamoah E. 2002. Functional organization of the neocortex in the congenitally deaf mouse. *Soc Neurosci Abstr* 533:538.
- Jones EG. 1985. *The thalamus*. New York: Plenum Press.
- Kahn DM, Krubitzer L. 2002. Massive cross-modal cortical plasticity and the emergence of a new cortical area in developmentally blind mammals. *Proc Natl Acad Sci USA* 99:11429–11434.
- Kalil RE, Schneider GE. 1975. Abnormal synaptic connections of the optic tract in the thalamus after midbrain lesions in newborn hamsters. *Brain Res* 100:690–698.
- Kanaka C, Ohno K, Okabe A, Kuriyama K, Itoh T, Fukuda A, Sato K. 2001. The differential expression patterns of messenger RNAs encoding K-Cl cotransporters (KCC1,2) and Na-K-2Cl cotransporter (NKCC1) in the rat nervous system. *Neuroscience* 104:933–946.
- Kaplan M, Mount D, Delpire E, Gamba G, Hebert S. 1996. Molecular mechanisms of NaCl cotransport. *Annu Rev Physiol* 58:649–668.
- Katz L, Shatz C. 1996. Synaptic activity and the construction of cortical circuits. *Science* 247:1133–1138.
- Kicliter E, Bruce L. 1983. Ground squirrel ventral lateral geniculate receives laminated retinal projections. *Brain Res* 267:340–344.
- King A, Hutchings M. 1987. Spatial response properties of acoustically responsive neurons in the superior colliculus of the ferret: a map of auditory space. *J Neurophysiol* 57:596–624.
- King A, Jiang Z, Moore D. 1998. Auditory brainstem projections to the ferret superior colliculus: anatomical contribution to the neural coding of sound azimuth. *J Comp Neurol* 390:342–365.
- King A. 1999. Sensory experience and the formation of a computational map of auditory space in the brain. *Bioessays* 21:900–911.
- Klauer G, Burda H, Nevo E. 1997. Adaptive differentiations of the skin of the head in the subterranean rodent, *Spalax ehrenbergi*. *J Morphol* 233:53–66.
- Kozel PJ, Friedman RA, Erway LC, Yamoah EN, Liu LH, Riddle T, Duff JJ, Doetschman T, Miller ML, Cardell EL, Shull GE. 1998. Balance and hearing deficits in mice with a null mutation in the gene encoding plasma membrane Ca-ATPase isoform 2. *J Biol Chem* 273:18693–18696.
- Krubitzer L, Kaas J. 1987. Thalamic connections of three representations of the body surface in somatosensory cortex of grey squirrels. *J Comp Neurol* 265:549–580.
- Krubitzer L, Kahn DM. 2003. Nature versus nurture revisited: an old idea with a new twist. *Prog Neurobiol* 70:33–52.
- Lazar G. 1983. Retinal projections of the pigmented guinea pig. *Acta Biol Hung* 34:207–213.
- Levanen S, Jousmaki V, Hari R. 1998. Vibration-induced auditory cortex activation in a congenitally deaf adult. *Curr Biol* 8:869–872.
- LeVay S, Wiesel TN, Hubel DH. 1980. The development of ocular dominance columns in normal and visually deprived monkeys. *J Comp Neurol* 191:1–51.
- Ling C, Schneider G, Jhaveri S. 1998. Target-specific morphology of retinal axon arbors in the adult hamster. *Vis Neurosci* 15:559–579.
- Lugo N, Kicliter E. 1995. Do retinal ganglion cells project bilaterally in ground squirrels? *Brain Res* 673:161–164.
- Lund R, Lund J, Wise R. 1974. The organization of the retinal projection to the dorsal lateral geniculate nucleus in pigmented and albino rats. *J Comp Neurol* 158:383–404.
- Lyckman AW, Jhaveri S, Feldheim DA, Vanderhaeghen P, Flanagan JG, Sur M. 2001. Enhanced plasticity of retinorecipient projections in an ephrin-A2/A5 double mutant. *J Neurosci* 21:7684–7690.
- Major DE, Rodman HR, Libedinsky C, Karten HJ. 2003. Pattern of retinal projections in the California ground squirrel (*Spermophilus beecheyi*): anterograde tracing study using cholera toxin. *J Comp Neurol* 463:317–340.
- Malmierca M, Merchan M, Henkel C, Oliver D. 2002. Direct projections from the cochlear nuclear complex to auditory thalamus in the rat. *J Neurosci* 22:10891–10897.
- McLaughlin T, Torborg C, Feller M, O'Leary DDM. 2003. Retinotopic map refinement requires spontaneous retinal waves during a brief critical period of development. *Neuron* 40:1147–1160.
- Middlebrooks J, Knudsen E. 1984. A neural code for auditory space in the cat's superior colliculus. *J Neurosci* 4:2621–2634.
- Mikkelsen J. 1992. Visualization of efferent retinal projections by immunohistochemical identification of cholera toxin subunit B. *Brain Res Bull* 28:619–623.
- Nakagawa Y, O'Leary DDM. 2001. Combinatorial expression patterns of LIM-Homeodomain and other regulatory genes parcellate developing thalamus. *J Neurosci* 21:2711–2725.
- Neville H, Lawson D. 1987. Attention to central and peripheral visual space in a movement detection task: an event-related potential and behavioral study—II, congenitally deaf adults. *Brain Res* 405:268–283.
- Nordeen KW, Killackey HP, Kitzes LM. 1983. Ascending projections to the inferior colliculus following unilateral cochlear ablation in the neonatal gerbil, *Meriones unguiculatus*. *J Comp Neurol* 214:144–153.
- O'Leary DDM, Wilkinson D. 1999. Eph receptors and ephrins in neural development. *Curr Opin Neurobiol* 9:65–73.

- Pace AJ, Madden VJ, Henson OW Jr, Koller BH, Henson MM. 2001. Ultrastructure of the inner ear of NKCC1-deficient mice. *Hear Res* 156:17–30.
- Pallas SL, Hahm J, Sur M. 1994. Morphology of retinal axons induced to arborize in a novel target, the medial geniculate nucleus: I, comparison with arbors in normal targets. *J Comp Neurol* 349:343–362.
- Paxinos G, Watson C. 1998. The rat brain in stereotaxic coordinates. San Diego, CA: Academic Press.
- Paxinos G, Franklin K. 2001. The mouse brain in stereotaxic coordinates. San Diego, CA: Academic Press.
- Penn AA, Riquelme PA, Feller MB, Shatz CJ. 1998. Competition in retinogeniculate patterning driven by spontaneous activity. *Science* 279:2108–2112.
- Petry H, Agarwala S, May J. 1989. Striped pattern of labeling in ground squirrel superior colliculus following intraocular HRP injections. *Brain Res* 489:199–203.
- Pham T, Rubenstein J, Silva A, Storm D, Stryker M. 2001. The CRE/CREB pathway is transiently expressed in thalamic circuit development and contributes to refinement of retinogeniculate axons. *Neuron* 31:409–420.
- Punj M, Hunt DL, Krubitzer L, Yamoah E. 2002. Cortical and subcortical connections of the inferior colliculus in the congenitally deaf mouse. *Soc Neurosci Abstr* 53:310.
- Reese B, Cowey A. 1983. Projection lines and the ipsilateral reintergeniculate pathway in the hooded rat. *Neuroscience* 10:1233–1247.
- Reese B, Cowey A. 1987. The crossed projection from the temporal retina to the dorsal lateral geniculate nucleus in the rat. *Neuroscience* 20:951–959.
- Röder B, Rosler F, Neville HJ. 1999. Effects of interstimulus interval on auditory event-related potential in congenitally blind and normally sighted humans. *Neurosci Lett* 264:53–56.
- Röder B, Rosler F, Neville HJ. 2000. Event-related potentials during auditory language processing in congenitally blind and sighted people. *Neuropsychologia* 38:1482–1502.
- Roe AW, Garraghty PE, Esguerra M, Sur M. 1993. Experimentally induced visual projections to the auditory thalamus in ferrets: evidence for a W cell pathway. *J Comp Neurol* 334:263–280.
- Ruthazer E, Cline H. 2004. Insights into activity-dependent map formation from the retinotectal system: a middle-of-the-brain perspective. *J Neurobiol* 59:134–146.
- Sadato N, Pascual-Leone A, Grafman J, Ibanex I, Deiber MP, Dold G, Hallett M. 1996. Activation of the primary visual cortex by Braille reading in blind subjects. *Nature* 380:526–528.
- Sadka R, Wollberg Z. 2004. Response properties of auditory activated cells in the occipital cortex of the blind mole rat: an electrophysiological study. *J Comp Physiol* 190:403–413.
- Schmidt J. 2003. Activity-driven sharpening of the retinotectal projection: the search for the retrograde synaptic signaling pathways. *J Neurobiol* 59:114–133.
- Schneider GE. 1973. Early lesions of the superior colliculus: factors affecting the formation of abnormal retinal projections. *Brain Behav Evol* 8:73–109.
- Shatz CJ. 1983. The prenatal development of the cat's retinogeniculate pathway. *J Neurosci* 3:482–499.
- Shatz CJ. 1996. Emergence of order in visual system development. *J Physiol Paris* 90:141–150.
- Sretavan D, Shatz C. 1986. Prenatal development of retinal ganglion cell axons: segregation into eye-specific layers within the cat's lateral geniculate nucleus. *J Neurosci* 9:171–207.
- Stauffer TP, Guerini D, Celio MR, Carafoli E. 1997. Immunolocalization of the plasma membrane Ca^{2+} pump isoforms in the rat brain. *Brain Res* 748:21–29.
- Sur M, Garraghty PE, Roe AW. 1988. Experimentally induced visual projections into auditory thalamus and cortex. *Science* 242:1437–1441.
- Sur M, Angelucci A, Sharma J. 1999. Rewiring cortex: the role of patterned activity in development and plasticity of neocortical circuits. *J Neurobiol* 41:33–43.
- Uchiumi O, Sugita S, Fukuta K. 1995. Retinal projections to the subcortical nuclei in the Japanese field vole (*Microtus montebelli*). *Exp Anim* 44:193–203.
- Weeks R, Horwitz B, Aziz-Sultan A, Tian B, Wessinger M, Cohen LG, Hallett M, Rauschecker JP. 2000. A positron emission tomographic study of auditory localization in the congenitally blind. *J Neurosci* 20:2664–2872.
- Winer JA, Chernock ML, Larue DT, Cheung SW. 2002. Descending projections to the inferior colliculus from the posterior thalamus and the auditory cortex in rat, cat, and monkey. *Hear Res* 168:181–195.
- Yamoah EN, Lumpkin EA, Dumont RA, Hudspete J, Gillespie PG. 1998. Plasma membrane Ca^{2+} -ATPase extrudes Ca^{2+} from hair cell stereocilia. *J Neurosci* 18:610–624.